Studies of laser-generated ultrasound using a micromachined silicon electrostatic transducer in air

William M. D. Wright
Department of Engineering, University of Warwick, Coventry CV4 7AL, United Kingdom

David W. Schindel
Department of Physics, Queens University, Kingston, Ontario K7L 3N6, Canada

David A. Hutchins
Department of Engineering, University of Warwick, Coventry CV4 7AL, United Kingdom

(Received 7 August 1993; accepted for publication 20 January 1994)

An air-coupled micromachined silicon electrostatic transducer has been used to detect ultrasound generated by a pulsed laser in metals and polymers. Bulk longitudinal and shear wave modes have been observed, as have Rayleigh waves in thick samples and Lamb waves in thinner plates. The results are in good agreement with surface displacement waveforms obtained using a contact capacitance device as a reference. The result is a flexible noncontact ultrasonic system with potential uses in materials characterization.

PACS numbers: 43.58.Vb, 43.38.Bs, 43.35.Yb

INTRODUCTION

Many situations occur in ultrasonic nondestructive testing where contact between transducer and sample is either undesirable or impossible, for example when the item to be tested is moving, hot or both. Several noncontact transduction techniques have been described in the literature, including optical methods,[1,2] electromagnetic acoustic transducers (EMATs),[3] capacitance transducers,[4] and others involving transmission and reception of the ultrasonic signal using air as the coupling medium.[5]

EMATs are able to generate and detect eddy currents, and are very simple devices consisting of a magnet and an rf coil. They are relatively insensitive, however, and are limited to electrically conductive materials such as metals at small stand-off distances (typically a few millimeters or less). These latter limitations are also shared by capacitance transducers which detect surface motion directly.

To enable noncontact transduction at a variety of solid surfaces, recent work has investigated optical methods for both generation and detection of ultrasonic transients. One attraction of such an approach is that an optical beam can be scanned easily and rapidly over the surface of an object. A pulsed laser is usually used for ultrasonic generation,[6,7] with detection based on some form of interferometry or laser beam deflection.[8] Many combinations are possible,[9] with recent applications including the inspection of large areas of a fiber reinforced polymer composite,[10] and the testing of hot metals.[11] A pulsed laser generates ultrasound using one of several possible mechanisms. In thermoelastic generation, the absorption of optical energy causes rapid thermal expansion, and hence ultrasonic generation occurs with a characteristic displacement waveform at the normal to the generation surface which contains a large shear component. Alternatively, the laser can be focused to produce an increased optical power density at the generation surface. Under such conditions, material ablation leads to a source with a displacement waveform dominated by a large monopolar longitudinal signal, and a smaller shear transient. A similar result is obtained by the evaporation of a fluid coating from the surface of the sample. Surface (Rayleigh) waves in thick samples, and guided modes (Lamb waves) in thin plates, can also be produced using these mechanisms.

There are some situations where the use of optical techniques for ultrasonic detection is not ideal (e.g., at very rough and nonreflective surfaces). In these situations it may be more practical to use more conventional transducers that use air as a coupling medium. Several types of air-coupled transducer exist. Composite piezoelectric transducers consist of piezoceramics such as PZT (lead–zirconate–titanate) which have been impedance matched to air to improve their efficiency. This can be achieved by machining grooves in the ceramic and filling them with epoxy,[12,13] leading to structures such as 1–3 connectivity composites. These can be tailored to have optimal electrical and mechanical properties for operation in air as either sources or receivers. An alternative design uses piezoceramic/polymer laminates.[14] In either case, impedance matching layers[15] tend to be used, to enhance transmission across the air/transducer boundary. Examples include thin layers of Lucite for composite devices[12] and compacted air-filled miniature spheres ("solid air") for conventional piezoelectric ceramics.[16] These types of transducer tend to have a narrow bandwidth and are usually resonant, although damping may be introduced via a suitable backing layer to increase bandwidth at the expense of sensitivity.

An alternative design involves the use of piezopolymer foil transducers,[17] which are manufactured using polyvinylidene fluoride (PVDF) polymer film or copolymers of, for example, vinylidene fluoride (VDF) and trifluoroethylene (TRFE).[18] Piezopolymers are better matched to air than ceramics and their relatively low mass gives them a

 0001-4966/94/95(5)/2567/9/$6.00

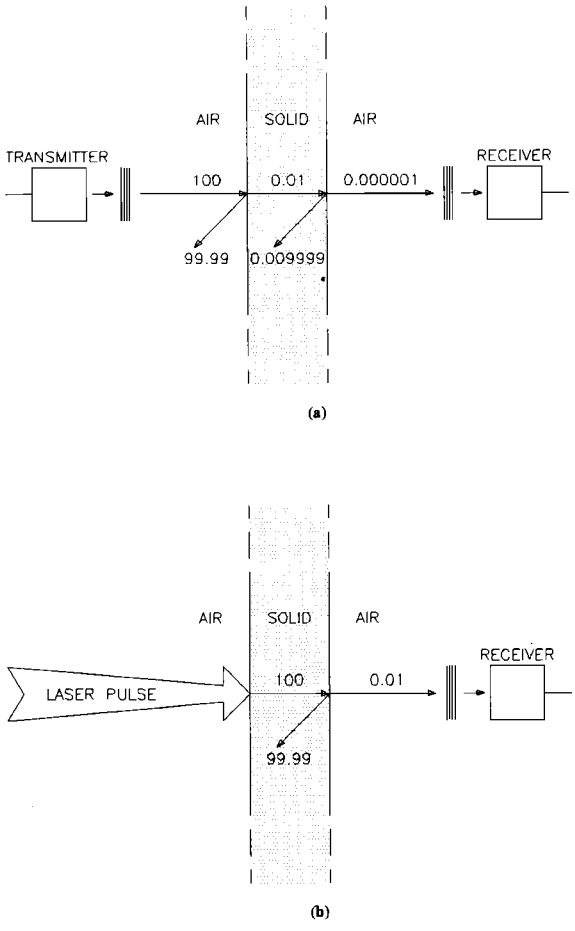

FIG. 1. (a) Through transmission in air using two air-coupled devices. (b) Improved transmission in air using a pulsed laser.

wide bandwidth. Their mechanical flexibility also allows curved and array transducers to be manufactured with relative ease.[19]

Recent research has also involved the investigation of electrostatic or capacitance transducers.[20] These consist of a metallized polymer membrane, stretched over a roughened backplate electrode to which a bias voltage is usually applied. When used as a detector, motion of the membrane causes variations in the electric field between the electrodes and thus also in the effective charge on the electrodes, which may then be detected using a charge sensitive amplifier. In generation, a driving voltage applied to the rigid backplate causes motion of the membrane. The quantity and dimensions of the air pockets formed between the roughened backplate and membrane appear to dictate the beam profile, frequency response, and sensitivity of the device.[21] The majority of the backplate electrodes reported in the literature are metallic, and are roughened by mechanical means, producing nonuniform surfaces and devices which are difficult to construct with reproducible characteristics. Despite these drawbacks, these devices give a good response in air at frequencies of up to 1 MHz, and have received recent interest for use in air-coupled transducer arrays for imaging and range-finding applications.[22] Recent work has attempted to improve reproducibility, sensitivity, and bandwidth by investigating the use of back-

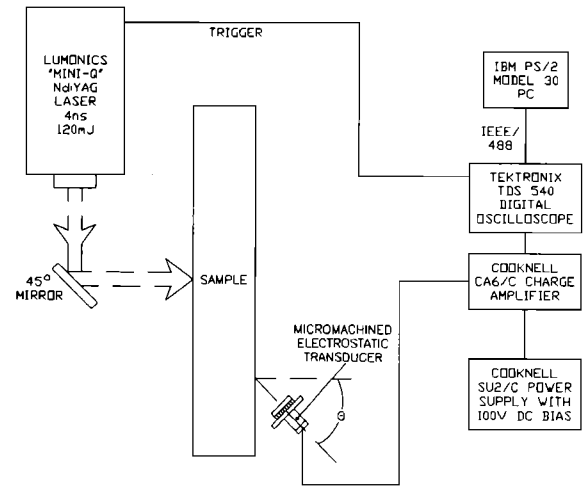

FIG. 2. Schematic diagram of the apparatus using the electrostatic air transducer.

plates fabricated from silicon.[23–27] Due to the uniformity of this silicon electrode and the accuracy and repeatability of integrated circuit manufacturing techniques, this form of device can be easily standardized. Such a design is used in this paper, and further details are given below.

The impedance mismatch between solid materials and air is probably the main reason why air-coupled ultrasonic applications appear to be restricted to areas such as range finding, surface profiling, and object identification, where reflection from an air/solid interface is used. If, however, it is required to couple ultrasound into a material (e.g., for material characterization), then the situation becomes more problematic. The intensity transmission coefficient at normal incidence across a boundary between two materials with different acoustic properties is given by the well-known equation[28]

$$\alpha_t = 4Z_1Z_2/(Z_1+Z_2)^2, \tag{1}$$

where α_t is the dimensionless transmission coefficient and Z_1, Z_2 are the specific acoustic impedances of the two materials, given by

$$Z_n = \rho_n c_n, \tag{2}$$

where ρ_n and c_n are the density and acoustic velocity of the material.

The value of α_t at an air/solid boundary is of the order of 0.0001 for most materials, and with such low transmission coefficients, measurement of material properties using

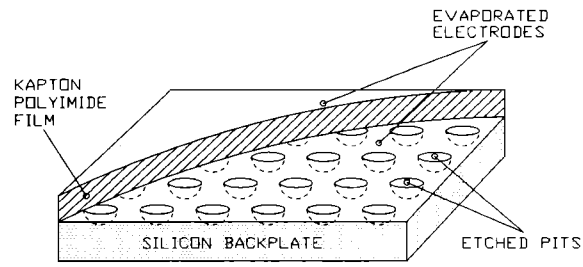

FIG. 3. Schematic diagram of the electrostatic air coupled transducer.

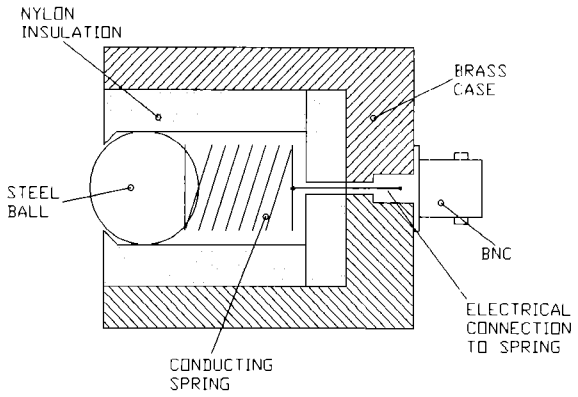

FIG. 4. Schematic diagram of the contact capacitance transducer.

air-coupled ultrasound is therefore difficult. Consider the scenario shown in Fig. 1(a), in which ultrasound is generated in air, passes through a solid material (e.g., aluminum), and is then detected in air on the opposite side. Only a small fraction of the original acoustic energy is transmitted through both air/solid interfaces to reach the receiver (the values shown are percentages). Now consider the second scenario shown in Fig. 1(b), in which the ultrasound is generated directly in the solid material using a pulsed laser. One of the interfaces with air has effectively been removed, so that now far more of the original acoustic energy reaches the receiver, making material characterization in air more feasible. In addition, a laser source is able to generate a multitude of different waves in a material. The work described here uses this arrangement to detect various laser generated acoustic waves in a number of materials using a silicon-based electrostatic device as a detector.

I. APPARATUS AND EXPERIMENT

Initial experiments were performed to detect laser-generated waveforms in a variety of solid materials, using both a micromachined silicon electrostatic transducer operating in air, and a standard broadband contact capacitance device. For the detection of longitudinal and shear waves, the equipment shown schematically in Fig. 2 was used, with the transducer face parallel to the surface of the sample (i.e., $\theta=0°$), and the laser source directly in line with the detector. The laser used for these characterization experiments was a Lumonics "Mini-Q" Q-switched Nd:YAG operating at an optical wavelength of 1064 nm,

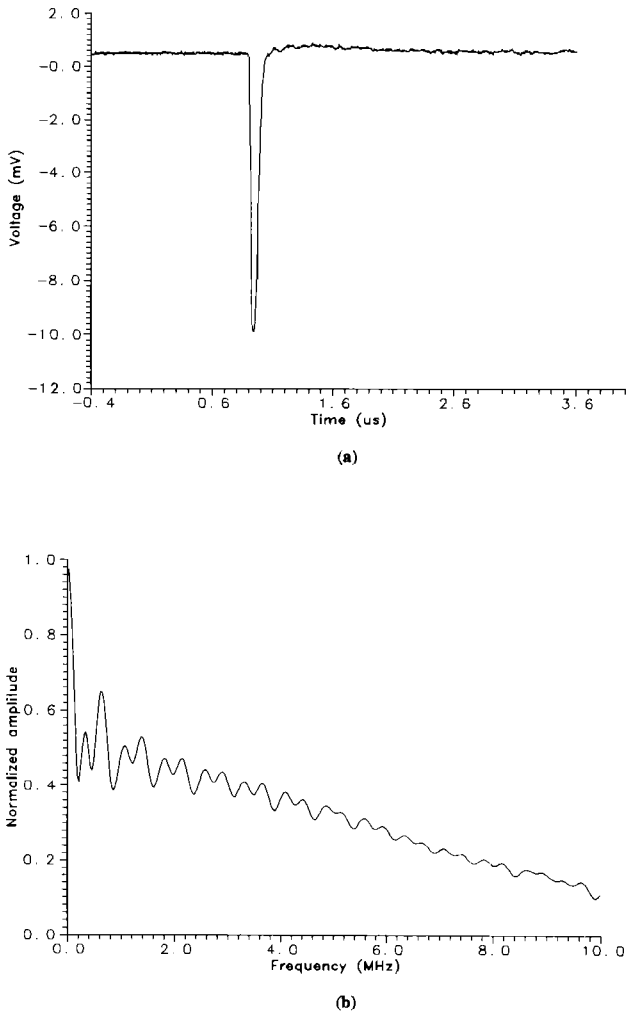

FIG. 5. (a) Longitudinal arrival in 44.0-mm aluminum using the contact capacitance device. (b) Frequency spectrum of (a).

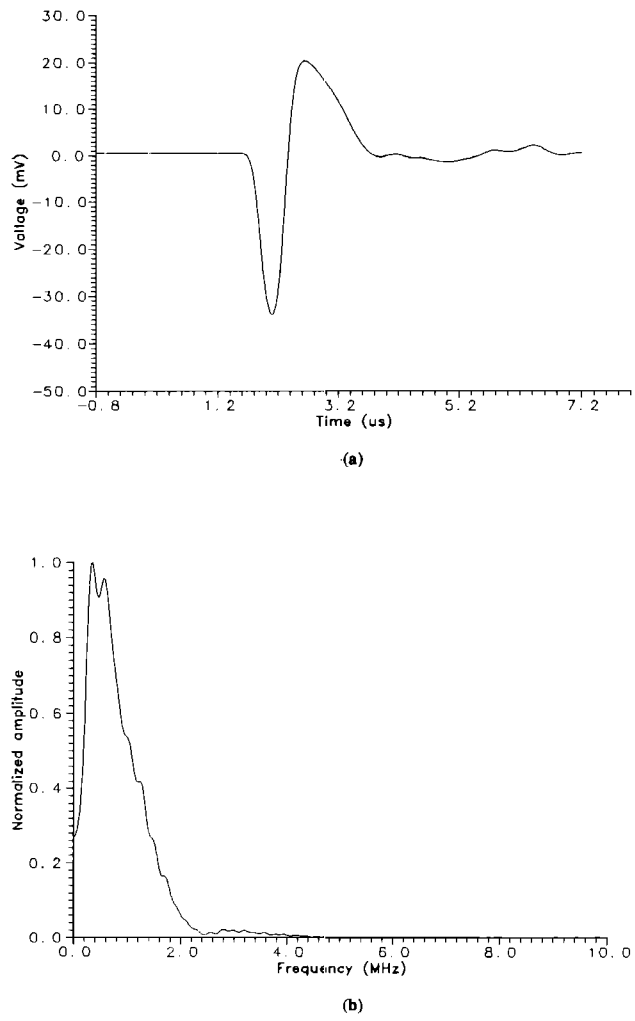

FIG. 6. (a) Longitudinal arrival in 44.0-mm aluminum using the air-coupled transducer. (b) Frequency spectrum of (a).

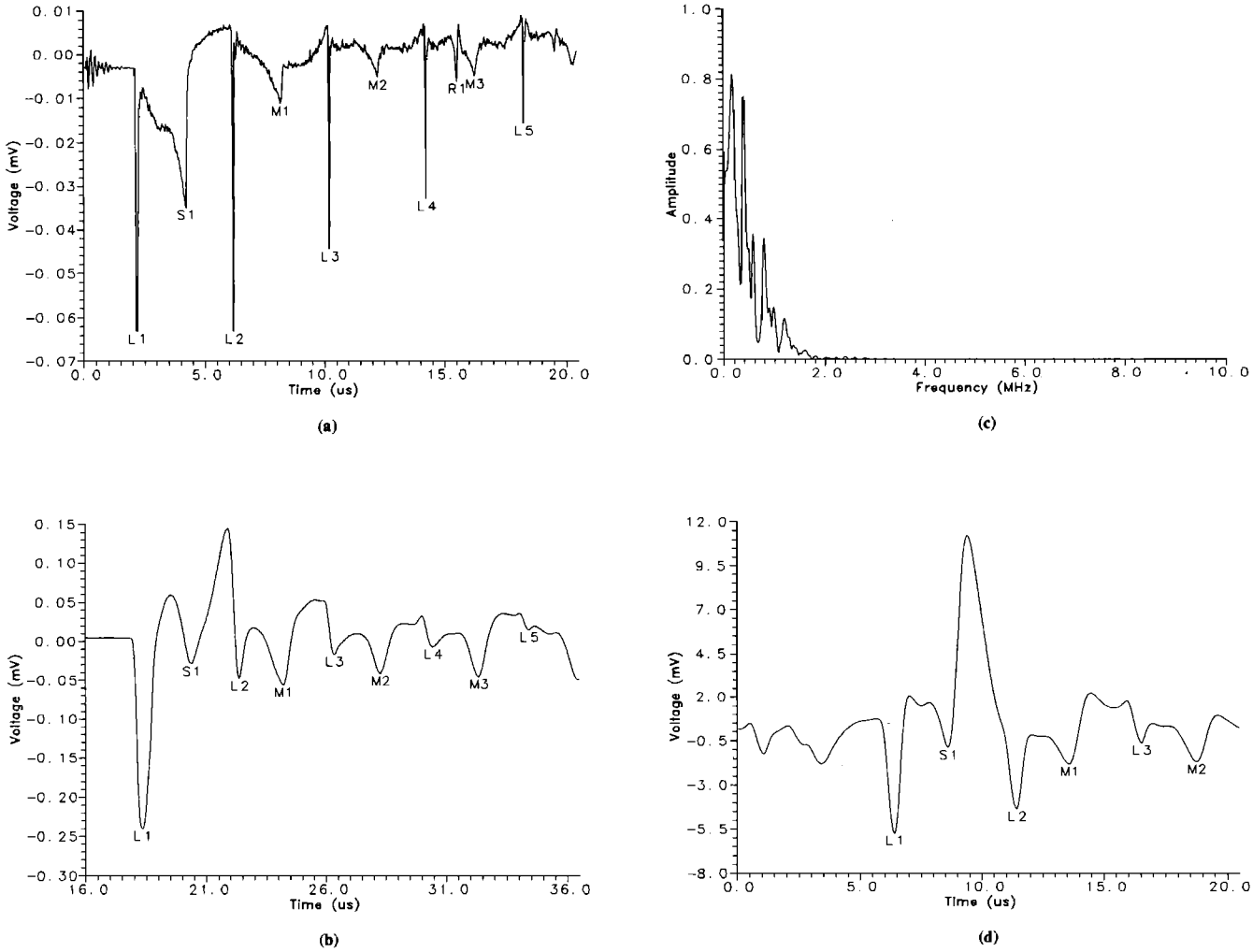

FIG. 7. (a) Signal in 12.83-mm aluminum using the contact capacitance transducer. (b) Signal in 12.83-mm aluminum using the electrostatic air transducer. (c) Modified frequency spectrum. (d) Waveform obtained from an inverse FFT of (c).

with a pulse duration of 4 ns and a maximum pulse energy of 120 mJ. This was directed onto an aluminum target to give an ablative source, the spot size being approximately 2 mm in diameter. Signals were then detected by the air-coupled electrostatic device, to which a dc bias of 100 V was applied via a Cooknell CA6/C charge amplifier with SU2/C power supply. The resultant time waveforms were captured using a Tektronix TDS 540 digital oscilloscope and transferred to an IBM PS/2 model 30 PC via an IEEE/488 interface for storage and analysis. In these experiments, a 5-mm air gap between the sample surface and the transducer was used, although much larger separations are possible.

The construction of the air-coupled device is shown schematically in Fig. 3. It used a silicon wafer into which small pits 40 μm in diameter, 80 μm apart, and approximately 30 μm deep had been anisotropically etched. A thin gold electrode was then evaporated onto the silicon, over which the metallized polymer film (7.5-μm "Kapton" polyimide) was placed. The applied bias voltage draws the film tightly over the etched pits causing them to behave in a similar way to miniature drum skins. The device used here had dimensions of 10×7 mm, and could act as both a transmitter and receiver of ultrasonic transients, but in these experiments it was acting as a receiver only.

To characterize the waveforms detected by the silicon transducer in air, waveforms were also detected for similar generation conditions using a contacting capacitance transducer, using the aluminum sample as one electrode (earthed), and a steel sphere in an insulated brass case as the second electrode, as shown in Fig. 4. This form of capacitance device has been well documented, and is known to be a broadband displacement sensor.[4] A household polymer film of 5 μm thickness was used as the dielectric between the two electrodes. Experiments were performed by simply replacing the micromachined silicon electrostatic air device with the contacting capacitance transducer, using the same bias voltage/charge amplifier unit and digital waveform recording facilities.

In addition to bulk modes transmitted through a sample and into air on the opposite side, Rayleigh waves[29] generated on a thick solid sample were studied. These experiments used the apparatus shown previously in Fig. 2, but with the laser source and air-coupled detector on the same surface, and the detector inclined at some angle θ toward the source. This was to detect the energy radiated

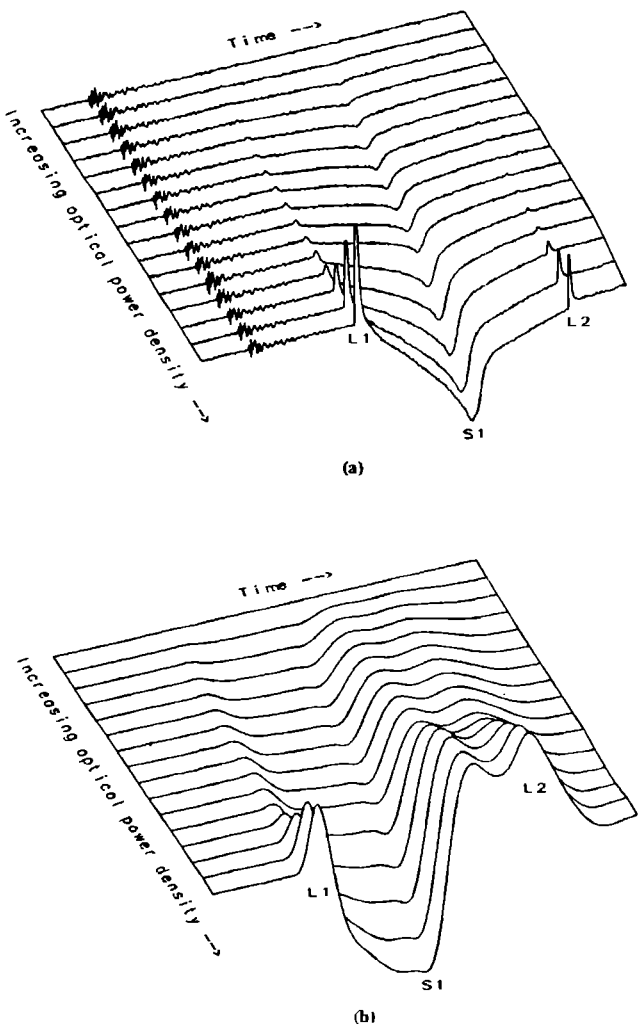

FIG. 8. (a) Varying optical power density waveforms for the contact capacitance device. (The waveforms have been inverted for presentation purposes.) (b) Varying optical power density waveforms for the electrostatic air transducer. (The waveforms have been inverted for presentation purposes.)

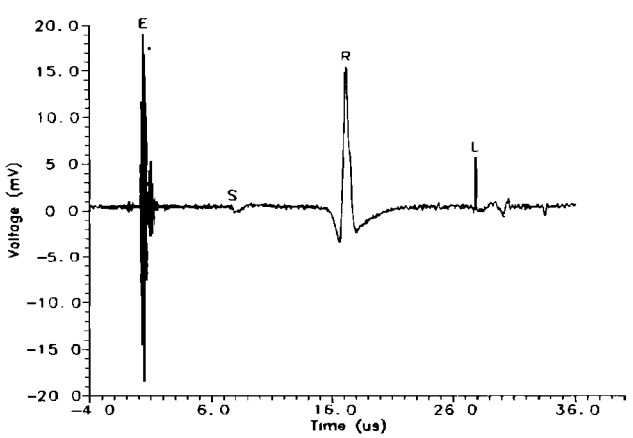

FIG. 9. Surface waves in aluminum using the contact capacitance transducer.

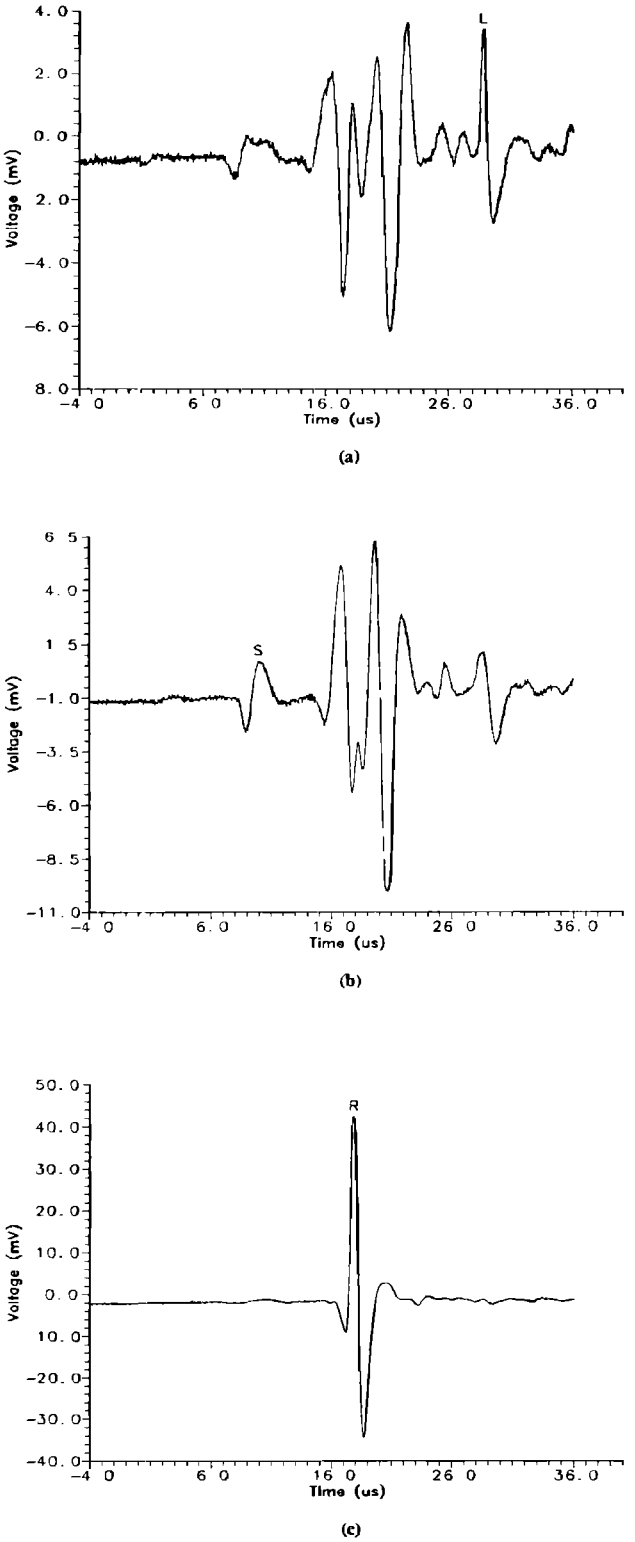

FIG. 10. (a) Surface waves in aluminum at $\theta=0°$ in air. (b) Surface waves in aluminum at $\theta=3°$ in air. (c) Surface waves in aluminum at $\theta=6°$ in air.

into air by the "leaky" Rayleigh wave, which is emitted at an angle given by Snell's law:

$$\frac{\sin \alpha_1}{\sin \alpha_2}=\frac{c_1}{c_2}, \tag{3}$$

where α is the angle the wave makes with the boundary, c is the velocity in material 1 (the solid) and 2 (air). For

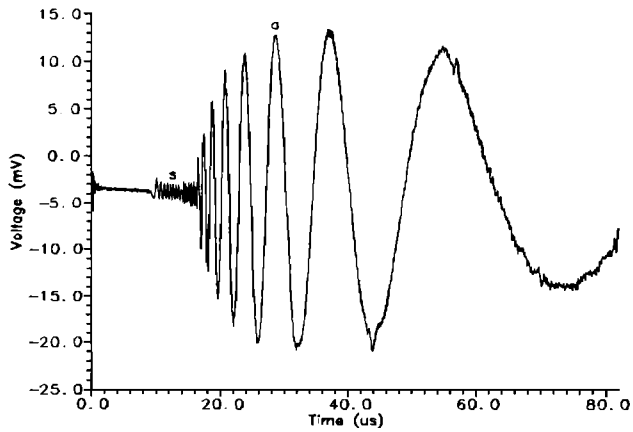

FIG. 11. Lamb waves in 0.69-mm aluminum using the contact capacitance device.

surface waves, $\alpha_1=90°$, and so the angle θ at which a surface wave radiates into air is simply

$$\theta=\sin^{-1}[c_2/c_1]. \tag{4}$$

The air-coupled device was only able to look at one angle (i.e., one value of θ) at a time, and hence there was expected to be an optimum angle for detection of a given feature having a certain velocity. As before, comparisons could be made to the normal displacement waveform, detected by the contacting capacitance transducer of Fig. 4.

Plate waves (Lamb waves)[29] may also be generated by a laser source in thin plates. These waves are dispersive and hence waves of different frequencies travel at different velocities in the same material. This also means that the different frequencies radiate or "leak" into air at different angles. Lamb waves exist in two sets of modes, symmetric and asymmetric. There are various orders within each set of modes, but if the plate thickness t is small enough, then only two modes exist, the zero-order symmetric (s_0) and asymmetric (a_0) modes. At low frequencies, the phase velocity of the symmetric modes will tend toward a single value known as the sheet velocity, which is slightly less than the longitudinal wave velocity for the material. The a_0 mode becomes highly dispersive, however, with low frequencies traveling at lower phase velocities. To detect such modes, the air-coupled electrostatic device can be pläced at some angle to the sample (a thin plate) as shown in Fig. 2, but because of dispersion effects the recorded signal is expected to be a strong function of the angle θ.

II. RESULTS AND DISCUSSION

A. Longitudinal and shear signals

The first experiments compared the signals detected by the silicon electrostatic transducer, using the configuration shown earlier in Fig. 2, with those of normal displacement of an aluminum surface for bulk mode propagation, detected by the contacting capacitance device of Fig. 4. The surface motion recorded in a 44-mm-thick aluminium plate for an ablative source (longitudinal arrival only) from the capacitance transducer is shown in Fig. 5(a). To illustrate the bandwidth present in this signal, a fast Fourier transform (FFT) of this signal was calculated, the result being presented in Fig. 5(b). This indicates that the contacting capacitance device was a broadband displacement sensor up to at least 10 MHz, which was also the upper frequency limit of the charge amplifier. The corresponding waveform for the electrostatic air transducer is shown in Fig. 6(a), with the FFT of the longitudinal arrival shown in Fig. 6(b). This indicates that the air transducer has a narrower bandwidth, with a reduced response at both low and high frequencies, when compared to the contact capacitance device. This may be attributed in part to the attenuation of high frequencies in air, as well as the different characteristics of the transducer, such as its larger active area. In addition, the applied bias voltage was limited by the charge amplifier to 100 V, and so the increased bandwidth which may be obtained by applying bias voltages of up to 400 V could not be used.[27]

A more typical waveform showing multiple echoes within a thinner (12.83 mm) sample of aluminum is shown in Fig. 7(a) using the contact capacitance transducer. Here, $L1$, etc. are the longitudinal wave arrivals, $S1$ is the first shear wave arrival, and $M1$, etc. are the mode converted shear waves formed from the reflection of a longitudinal wave from a metal/air interface. The feature $R1$ is a reflection from the edge of the sample. Figure 7(b) shows the corresponding signal from the electrostatic air transducer, and there is excellent correlation between the two, with all the main features ($L1$,$S1$,$M1$, etc.) seen in the contact transducer waveform clearly visible in the air coupled waveform. It is difficult, however, to deduce from these results whether the electrostatic device is a displacement or a velocity sensor. The signal in Fig. 6(a) is the response of the air transducer to what is essentially a delta function from the laser, and hence the spectrum shown in Fig. 6(b) may be thought of as the overall frequency response of the device. If the FFT of the contact capacitance device waveform containing multiple echoes shown in Fig. 7(a) is multiplied by the FFT shown in Fig. 6(b) of the air transducer response, the frequency spectrum shown in Fig. 7(c) is produced. The waveform corresponding to this spectrum can be obtained using an inverse FFT, with the result shown in Fig. 7(d). This is, in effect, the surface displacement waveform Fig. 7(a) filtered over the restricted range of frequencies detected by the air transducer. Comparison of Fig. 7(d) to the air transducer waveform containing multiple echoes, Fig. 7(b), demonstrates a high degree of similarity, and so it would be reasonable to assume that the electrostatic device may be approximated to a displacement sensor with a reduced bandwidth, rather than a velocity sensor.

Another experiment was carried out in which the optical power density at the aluminum surface produced by the laser source was gradually increased, so that the generation mechanism changed from thermoelastic expansion to ablation. A selection of waveforms is presented in Fig. 8(a) for the contact capacitance device and Fig. 8(b) for the air-coupled electrostatic transducer. Again there is good correlation between the two devices. The steplike

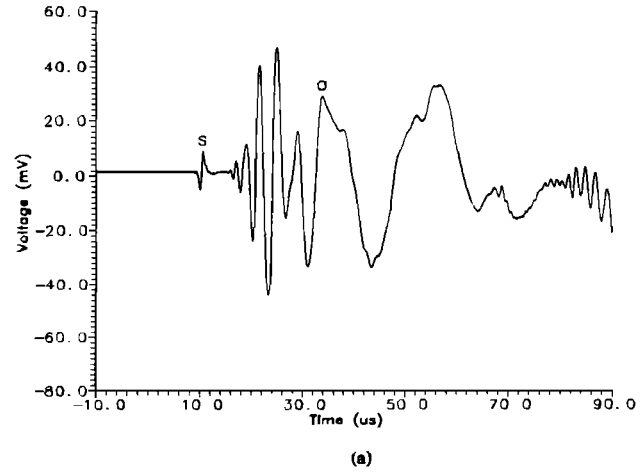

(a)

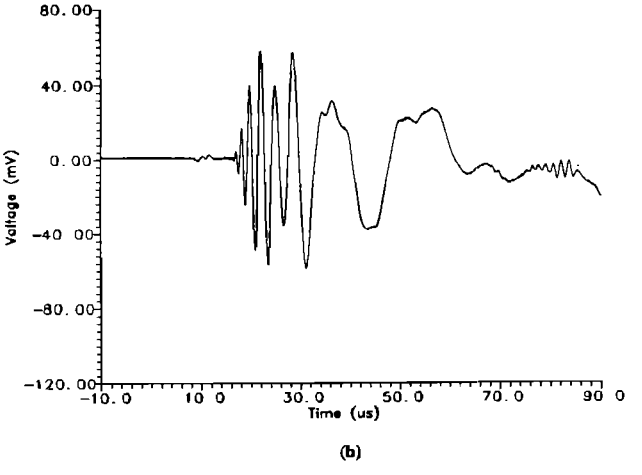

(b)

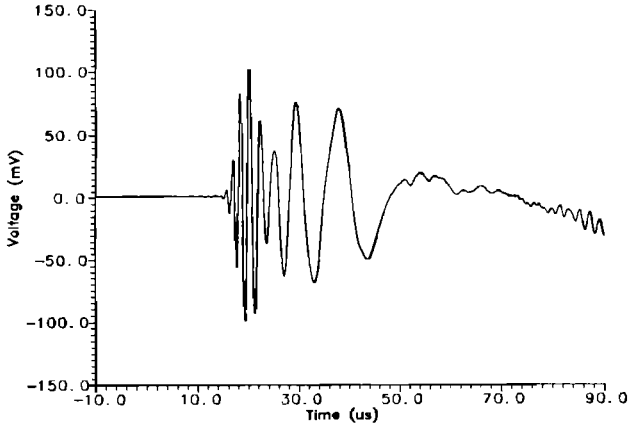

(c)

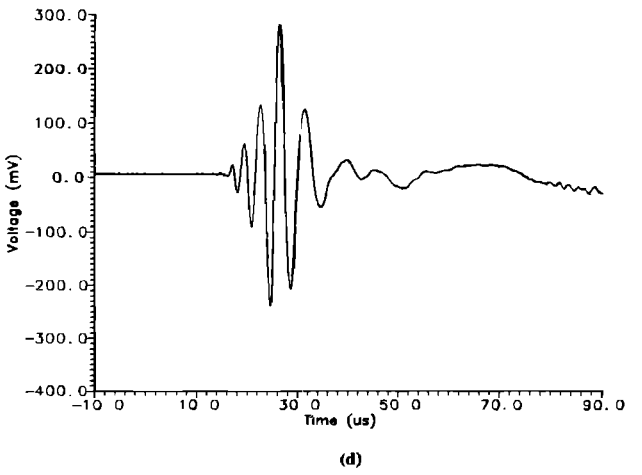

(d)

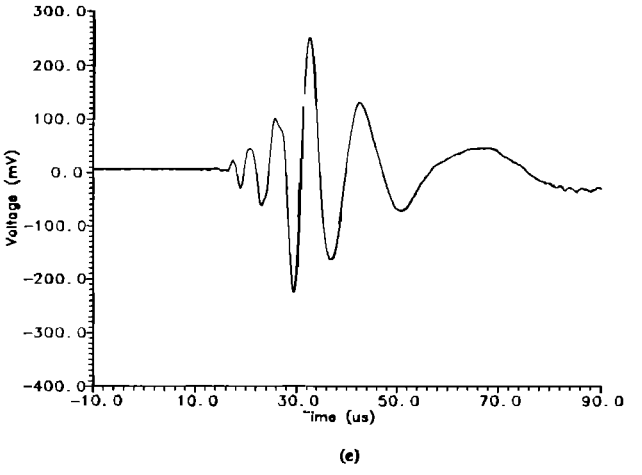

(e)

FIG. 12. (a) Lamb waves in 0.69-mm aluminum at $\theta=2°$ in air. (b) Lamb waves in 0.69-mm aluminum at $\theta=5°$ in air. (c) Lamb waves in 0.69-mm aluminum at $\theta=10°$ in air. (d) Lamb waves in 0.69-mm aluminum at $\theta=15°$ in air. (e) Lamb waves in 0.69-mm aluminum at $\theta=20°$ in air.

shear arrival $S1$ is present in most of the waveforms, and the monopolar longitudinal arrival $L1$ and it's echo $L2$ increasingly dominate the signal as the source becomes more ablative.

Similar results were also obtained in samples of brass and steel, with variations due to differences in microstructure, thermal characteristics, and elastic properties. Waveforms were also obtained in polymethylmethacrylate ("Plexiglass" or "perspex") samples by replacing the Nd:YAG laser with a Lumonics "Lasermark" series model 630 CO_2 TEA laser, which had a pulse duration of 100 ns and a maximum energy of 8 J. This operated at an optical wavelength of 10.6 μm, in the far infrared, where absorption in this polymer, which transmits visible and near infrared light, is high. The waveforms displayed the same characteristics, but with a more prominent shear step due to improved thermoelastic generation.

B. Rayleigh and Lamb wave signals

As previously stated, surface waves (Rayleigh waves) are generated by a laser source at a solid surface simulta-

neously with bulk modes. The apparatus used was shown schematically earlier in Fig. 2, using the Nd:YAG laser and both the air-coupled device and the contacting capacitance transducer in turn on the same side of an aluminum sample 180 mm diam and 86.0 mm thick. A typical normal displacement waveform as detected by the contacting capacitance transducer is shown in Fig. 9. Feature E is the electrical feedthrough from the laser, and is in effect a noise signal, S is a surface skimming longitudinal wave, R is the Rayleigh wave traveling at slightly less than the bulk shear wave velocity, and L is the first longitudinal wave echo within the block thickness. The experiment was then repeated using the air coupled transducer, with results for various values of θ (the angle the transducer makes with the surface normal), being shown in Fig. 10. The different wave types radiate into the air at different angles depending on their velocity, as dictated by Snell's law in Eq. (4), and hence detection of the annotated features by the air transducer could be optimized by varying θ, as shown for (a) the longitudinal wave L ($\theta=0°$), (b) the surface skimming wave S ($\theta=3°$), and (c) the Rayleigh wave R ($\theta=6°$).

Lamb waves were detected using the arrangement shown earlier in Fig. 2, initially with the contact capacitance transducer displaced 50 mm laterally from the Nd:YAG laser source. A 300×300 mm plate of 0.69-mm-thick aluminum was used, and a typical normal displacement waveform obtained is shown in Fig. 11. The zero-order symmetric (s_0) and asymmetric (a_0) modes are clearly visible. Both modes show some dispersion, due to the thickness of the plate and the range of frequencies present, but this is more prominent in the a_0 mode, as would be expected for the dispersion relations for these modes in thin plates.

By replacing the contact device with the electrostatic air transducer, the various Lamb modes could be detected in air. A selection of waveforms at different angles of the detector (θ in Fig. 2) is shown in Fig. 12(a) to (e). At $\theta=2°$, the symmetric mode s is clearly visible, but reduces in amplitude at $\theta=5°$, and is not present at 10°. This is to be expected, as the s_0 mode in thin plates has a velocity approaching the sheet (i.e., longitudinal) velocity, and hence will radiate into air at small angles. The higher frequency asymmetric vibrations become more prominent at $\theta=5°$–10°, and at higher angles the frequency content of this asymmetric mode clearly decreases. Lamb waves were also generated and detected in a 1.5-mm-thick plate of polymethylmethacrylate ("Plexiglass" or "perspex") using the CO_2 laser described previously as the ultrasonic source. These also displayed the same features, namely the initial s_0 mode signal, followed by the highly dispersive a_0 mode.

III. CONCLUSIONS

Experiments have been performed in which laser-generated ultrasonic waves have been detected using a micromachined electrostatic air transducer. Longitudinal and shear arrivals have been observed in aluminum, brass, and steel, surface waves in aluminum, and Lamb waves in thin plates of aluminum and polymethylmethacrylate ("Plexiglass" or "perspex"). The response of this transducer has been compared with that of a contact capacitance device which is a known broadband surface displacement sensor, and it appears that the electrostatic device is also a displacement sensor with a reduced bandwidth. The flexibility of this hybrid system has been demonstrated, and it should find use in many applications where contact with a material needs to be avoided.

[1] J.-P. Monchalin, "Optical detection of ultrasound," IEEE Trans. Ultrason. Ferroelec. Freq. Control UFFC-33, 485–499 (1986).

[2] C. B. Scruby and L. E. Drain, *Laser Ultrasonics: Techniques and Applications* (Hilger, Bristol, 1990).

[3] H. M. Frost, "Electromagnetic-Ultrasound Transducers: Principles, Practice and Applications," in *Physical Acoustics—Principles and Methods*, edited by W. P. Mason and R. N. Thurston (Academic, New York, 1979), Vol. XIV, pp. 179–275.

[4] W. Sachse and N. N. Hsu, "Ultrasonic Transducers for Materials Testing and Their Characterization," in *Physical Acoustics—Principles and Methods*, edited by W. P. Mason and R. N. Thurston (Academic, New York, 1979), Vol. XIV, pp. 277–406.

[5] W. Manthey, N. Kroemer, and V. Mágori, "Ultrasonic transducers and transducer arrays for applications in air," Meas. Sci. Tech. 3, 249–261 (1992).

[6] R. M. White, "Generation of elastic waves by transient surface heating," J. Appl. Phys. 34, 3559–3567 (1963).

[7] D. A. Hutchins, "Ultrasonic generation by pulsed lasers," in *Physical Acoustics—Principles and Methods*, edited by W. P. Mason and R. N. Thurston (Academic, New York, 1988), Vol. XVIII, pp. 21–123.

[8] B. Sullivan and A. C. Tam, "Profile of laser-produced acoustic pulse in a liquid," J. Acoust. Soc. Am. 75, 437–441 (1984).

[9] J. W. Wagner, "Optical detection of ultrasound," in *Physical Acoustics—Principles and Methods*, edited by W. P. Mason and R. N. Thurston (Academic, New York, 1990), Vol. XIX, pp. 201–266.

[10] J.-P. Monchalin, J.-D. Aussel, P. Bouchard, and R. Heon, "Laser-ultrasonics for industrial applications," in *Review of Progress in Quantitative NDE*, edited by D. O. Thompson and D. E. Chimenti (Plenum, New York, 1988), Vol. 7B, pp. 1607–1614.

[11] C. A. Calder and W. W. Wilcox, "Non-contact material testing using laser energy deposition and interferometry," Mater. Eval. 38, 86–91 (1980).

[12] T. R. Gururaja, W. A. Schulze, L. E. Cross, R. E. Newnham, B. A. Auld, and Y. J. Wang, "Piezoelectric composite materials for ultrasonic transducer applications. Part I: Resonant modes of vibration of PZT Rod-Polymer composites," IEEE Trans. Sonics Ultrason. SU-32, 481–498 (1985).

[13] J. A. Hossack and G. Hayward, "Finite-element analysis of 1-3 composite transducers," IEEE Trans. Ultrason. Ferroelec. Freq. Control UFFC-38, 618–629 (1991).

[14] P. Kleinschmidt and V. Mágori, "Ultrasonic robotic sensors for exact short range distance measurement," Proc. 1985 IEEE Ultrason. Symp. 457–462 (1985).

[15] L. C. Lynnworth, "Ultrasonic impedance matching from solids to gases," IEEE Trans. Sonics Ultrason. SU-13, 37–48 (1965).

[16] M. Teshigawara, F. Shibata, and H. Teramoto, "High resolution (0.2 mm) and fast response (2 ms) range finder for industrial use in air," Proc. 1989 IEEE Ultrason. Symp. 639–642 (1989).

[17] R. Lerch and G. M. Sessler, "Microphones with rigidly supported membranes," J. Acoust. Soc. Am. 67, 1379–1381 (1980).

[18] H. Ohigashi, K. Koga, M. Suzuki, and T. Nakanishi, "Piezoelectric and ferroelectric properties of P(VDF–TrFE) copolymers and their application to ultrasonic transducers," Ferroelectrics 60, 263–276 (1984).

[19] M. Platte, "PVDF ultrasonic transducers," Ferroelectrics 75, 327–337 (1987).

[20] H. Carr, W. S. H. Munro, M. Rafiq, and C. Wykes, "Developments in capacitive transducers," Nondest. Test. Eval. 10, 3–14 (1992).

[21] W. Kuhl, G. R. Schodder, and F.-K. Schröder, "Condenser transmitters and microphones with solid dielectric for airborne ultrasonics," Acustica 4, 519–532, (1954).

[22] H. Carr and C. Wykes, "Diagnostic measurements in capacitive transducers," Ultrasonics 31, 13–20 (1993).

[23] K. Suzuki, K. Higuchi, and H. Tanigawa, "A Silicon Electrostatic Ul-

trasonic Transducer," IEEE Trans. Ultrason. Ferroelec. Freq. Control UFFC-36, 620–627 (1989).
[24]D. W. Schindel and D. A. Hutchins, "Capacitance devices for the controlled generation of ultrasonic fields in liquids," Proc. IEEE 1991 Ultrason. Symp., 301–304 (1991).
[25]D. W. Schindel, D. A. Hutchins, L. Zou, and M. Sayer, "Capacitance devices for the controlled generation of air-borne ultrasonic fields," Proc. IEEE 1992 Ultrason. Symp., 843–846 (1992).
[26]D. W. Schindel, D. A. Hutchins, L. Zou, and M. Sayer, "Capacitance transducers for generating ultrasonic fields in liquids and gases," in *Proceedings of the IEE International Conference on Acoustic Sensing and Imaging* (IEE, London, 1993), conference publication No. 369, pp. 7–12.
[27]D. W. Schindel, D. A. Hutchins, L. Zou, and M. Sayer, "The design and characterization of micromachined air-coupled capacitance transducers", submitted to IEEE Trans. Ultrason. Ferroelec. Freq. Control.
[28]J. Blitz, *Fundamentals of Ultrasonics* (Butterworths, London, 1967), 2nd ed.
[29]I. A. Viktorov, *Rayleigh and Lamb Waves: Physical Theory and Applications* (Plenum, New York, 1967).